Structural and Multidisciplinary Optimization (2020) 62:193–207
https://doi.org/10.1007/s00158-019-02479-1

RESEARCH PAPER

Optimum target stiffness allocation for design of a reinforcing member on an existing structure

Shinyu Kim[1] · Saekyeol Kim[1] · Tae Hee Lee[1] · SeongWook Seo[2]

Received: 5 August 2019 / Revised: 18 November 2019 / Accepted: 12 December 2019 / Published online: 15 February 2020

Abstract

The reinforcing members are often added on an existing structure to improve stiffness of the structure up to required level. In general, the design targets for the reinforcing members need to be allocated for their designs. However, since the members are additively designed, it is difficult to predict behavior of the reinforcing members and their influence on the existing structure. Therefore, allocating the design targets is challenging task, and the targets based on engineering experience and intuition can lead to the repetitive design cycles. This paper proposes a method for determining target stiffness of a reinforcing member which makes an existing structure achieve the required performances. To utilize individual models of an existing structure and the reinforcing members in a design, the system of equations of the assembled structure is decomposed by using a substructuring technique. Additional boundary conditions are imposed on the interfaces between the structure and members to ensure consistency between models, and the target stiffness of the member is defined by using the boundary conditions. The optimal target stiffness and design of the members are determined through the use of a multidisciplinary design optimization technique, analytical target cascading. This method is applied to a simple portal frame and a body-in-white with reinforcing member of a vehicle manufactured by Hyundai Motor Company. By using the optimal target stiffness, reinforcing member of any shape can be designed independently and at little cost, without access of the existing structure model.

Keywords Target stiffness allocation · Reinforcing member · Structure reinforcement · Complex structure · Design optimization · Analytical target cascading

1 Introduction

When a structure undergoes certain changes, including a modification in use, the environment, regulations, or the operating conditions, the structure should be reinforced to deal with such alterations (Yang and Liang 2011). The changes to a structure can be dealt with by updating its shape, size, and material, but this is occasionally not cost-effective. Because the existing structure should be discarded, including the structure itself, and because of the added costs for the required design and manufacturing. Another way to utilize an existing structure without discarding it is by adding some specially designed reinforcing members, which can be easily found in vehicle structural designs. For example, vehicle manufacturers develop high-performance trim level vehicle models by adding reinforcing members on an existing body structure of a base trim level vehicle model. To achieve the ride and handling performance required for a high-performance vehicle, reinforcing members specialized for a specific stiffness of the vehicle are designed. Strut tower bars located underneath the hood are designed to improve the global torsional stiffness of the vehicle structure (Takamatsu et al. 1992). Lower tie bars mounted around the subframes are specially designed to improve the local stiffnesses of the suspension structure. By utilizing these reinforcing members, several models with different purposes can be developed under a reduced time frame and cost in terms of development and production.

When the design and model of an existing structure already exists, the design of the reinforcing members is

Responsible Editor: Jianbin Du

✉ Tae Hee Lee
thlee@hanyang.ac.kr

[1] Department of Automotive Engineering, Hanyang University, Seoul 04763, Korea

[2] High Performance Vehicle Body Engineering Design Team, HYUNDAI MOTOR, Hwaseong-si, Gyeonggi-do 18280, Korea

generally conducted individually by allocating stiffness targets. These targets allow the existing structure to satisfy the required stiffness level. For example, the stiffness, mass, durability, and natural frequency are allocated to the reinforcing members using target values. With these design targets, the design of the members can be rapidly conducted and reviewed, and a stand-alone design procedure of the reinforcing member can be achieved. However, because the members are additively and newly designed, it is difficult to identify their behavior in an assembled structure. Therefore, identifying the guidelines and targets is a challenging task, involving engineers to determine the targets based on their engineering experience and intuition. Because the targets are determined based on experience, the assembled structure may not satisfy the design requirements, and the optimality of the design cannot be guaranteed. If the design does not meet the requirements, the design targets are revised again using intuition, followed by repetitive design cycles (Austin-Breneman et al. 2012).

Because the problem consists of two disciplines, namely the existing structure and the reinforcing members, a multidisciplinary design optimization (MDO) can be a solution (Martins and Lambe 2013). MDO methods can be classified into two groups. The first, a multidisciplinary feasible (MDF) method, optimizes systems by uniting distributed subsystems through a multidisciplinary analysis (MDA). A bilevel integrated system synthesis (BLSS) (Sobieszczanski-Sobieski et al. 2000) and concurrent subspace optimization (CSSO) (Sobieszczanski-Sobieski 1988) are representative MDF methods. The other type is an individual discipline feasible (IDF) method, which achieves an optimization in a distributed environment. Collaborative optimization (CO) (Braun 1997), BLISS-2000 (Tosserams et al. 2010) and analytical target cascading (ATC) (Kim 2001) are representative IDF methods. Typical MDO methods focus on solving multidisciplinary systems consisting of pre-decomposed disciplines and specific linking variables between the disciplines. For example, ATC, which was developed to optimize hierarchical systems, can be used to derive a target value as a linking variable. The ATC method is widely used in the design of dynamic systems for which the disciplines can be easily decomposed (Kim et al. 2003, 2016; Kokkolaras et al. 2004). However, in contrast to dynamic systems, where linking variables between the components, such as stiffness coefficients and damping coefficients, are clearly defined, it is difficult to define linking variables between the structure and its members. Therefore, early research into the application of ATC to a static structure design defined the linking variables between components, such as the bending or torsional stiffness, based on the intuition of the engineers (Kang et al. 2014). However, because these linking variables, which were defined as a partial stiffness of substructures, cannot express the complete behavior of a substructure, it is difficult to guarantee the feasibility and optimality of the assembled structures. To derive an accurate target stiffness for a reinforcing member, the structural relation between the structure and members should be reviewed precisely through a system of equations.

This paper presents a method for determining target stiffness of a reinforcing member which makes an existing structure achieve required stiffness. To utilize individual models of an existing structure and a reinforcing member, a system of equations for each model is derived from the assembled structure using a substructuring technique. New boundary conditions are introduced at the interfaces between the structure and members to ensure consistency between individual models and to define the target stiffness of the reinforcing member. By utilizing each model as a discipline and the target stiffness as a linking variable, the optimal target stiffness allowing the assembled structure to satisfy the required stiffness is determined using ATC. Based on the derived target stiffness of the member, an independent design of a member of any shape, without access of a model of the existing structure, can be achieved while guaranteeing the stiffness of the assembled structure.

The remainder of this paper is organized follows: In Section 2, individual models and the target stiffness are derived from a system of equations of assembled structure by using a substructuring. In Section 3, an optimization scheme based on the ATC method is described to determine and allocate the optimal target stiffness of the member. In Section 4, examples are offered as an examination of the proposed method. First, a simple portal frame of a reinforcing member is employed as an example to analytically illustrate the proposed method. The method is then applied to the design of a reinforcing member of a vehicle body-in-white (BIW). The design problem and result of a reinforcing member on a vehicle are then described. Finally, some concluding remarks are given in Section 5.

2 Decomposition of structure and definition of target stiffness

Decomposed substructures offer design process advantages over assembled structures. Because a model of an existing structure already exists, it is more reasonable to build an individual model of new reinforcing member and utilize individual models in the design process. If they are combined into a single model, the model will become much more complex than before, and more cost will be required for an analysis. In addition, by deriving the design targets, reinforcing members can be designed independently, and an expensive model of the existing structure is no longer

required. This can reduce time and cost in individual design of the reinforcing member.

In this section, to utilize decomposed models, the existing structure and the reinforcing member are derived by decomposing system of equations of assembled structure. Additional boundary conditions (B.C.) are introduced on each model to achieve consistency between models. Based on the boundary conditions, the target stiffness of the reinforcing members is defined.

2.1 System of equations

An analysis of a structure can be classified according to the linearity of the behavior and the time-variance of the load. According to the linearity between the applied load and the deformation of the structure, an analysis can be classified into linear and non-linear approaches. Besides, according to the time-variance of the load applied to the structure, or a consideration of the inertia effect of the structure, an analysis can be classified as being static or dynamic. For general explanation, the proposed method is developed by using linear static model, which is most widely used (Adams 2008). Equation (1) shows the system of equations used for a linear static structure (Zienkiewicz et al. 1977).

$$\mathbf{K}\mathbf{u} = \mathbf{F} \tag{1}$$

where $\mathbf{K}$ represents the stiffness matrix of a structure and $\mathbf{u}$ represents the displacement of each structure node. In addition, $\mathbf{F}$ represents the external forces applied to each node.

For an easier explanation of the decomposition of the system of equations, a simple portal frame structure with a reinforcing member is introduced in Fig. 1. A member with a dashed line represents a reinforcing member, and a member with a solid line represents an existing structure. From the perspective of substructuring, because both are part of the assembled structure, the existing structure and the reinforcing member are called the upper and lower substructures, respectively. The prefixes "upper" and "lower" represent the relative vertical relationship of the substructures in the physical hierarchy of the structure. In

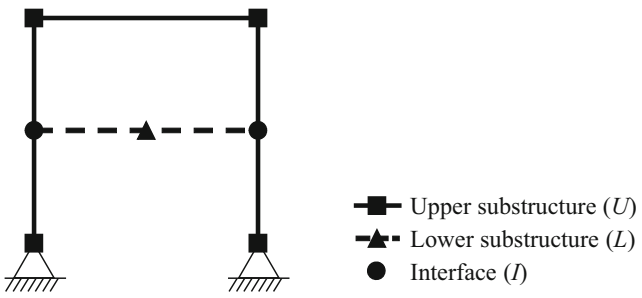

Fig. 1 Portal frame structure with reinforcing member

Section 2, an existing structure and a reinforcing member are referred to as upper and lower substructures to explain the substructuring procedure. Nodes can be classified into three groups according to where they belong: the upper substructure, the lower substructure, and interface between the upper and lower substructures. Each node is denoted as filled square, triangle, and circle in Fig. 1, respectively. Based on the classification of the nodes, a system of equation of assembled structures can be rewritten as follows:

$$\begin{bmatrix} \mathbf{K}_{UU} & \mathbf{K}_{UI} & 0 \\ \mathbf{K}_{IU} & \mathbf{K}_{II} & \mathbf{K}_{IL} \\ 0 & \mathbf{K}_{LI} & \mathbf{K}_{LL} \end{bmatrix} \begin{bmatrix} \mathbf{u}_U \\ \mathbf{u}_I \\ \mathbf{u}_L \end{bmatrix} = \begin{bmatrix} \mathbf{F}_U \\ \mathbf{F}_I \\ \mathbf{F}_L \end{bmatrix} \tag{2}$$

where subscripts represent the classification of nodes. U, I, and L represent the upper substructure, interface between the substructures, and the lower substructure, respectively. Since the nodes on interface are included in both members of the upper and lower substructures, $\mathbf{K}_{II}$ can be rewritten as follows (3):

$$\mathbf{K}_{II} = \mathbf{K}_{II}^{(U)} + \mathbf{K}_{II}^{(L)} \tag{3}$$

$\mathbf{K}_{II}^{(U)}$ is the partial stiffness matrix of interface nodes related to the upper substructure, and $\mathbf{K}_{II}^{(L)}$ is related to the lower substructure. The other stiffness matrices are solely dependent on the upper or lower substructure. $\mathbf{K}_{UU}$, $\mathbf{K}_{UI}$, and $\mathbf{K}_{IU}$ are related to the upper substructure, whereas $\mathbf{K}_{IL}$, $\mathbf{K}_{LI}$, and $\mathbf{K}_{LL}$ are related to the lower substructure. Based on the dependency of the stiffness matrix, the system of equations can be decomposed as (4) by introducing a new term, $\mathbf{F}_C$.

$$\begin{bmatrix} \mathbf{K}_{UU} & \mathbf{K}_{UI} \\ \mathbf{K}_{IU} & \mathbf{K}_{II}^{(U)} \end{bmatrix} \begin{bmatrix} \mathbf{u}_U \\ \mathbf{u}_I \end{bmatrix} = \begin{bmatrix} \mathbf{F}_U \\ \mathbf{F}_I - \mathbf{F}_C \end{bmatrix}$$
$$\begin{bmatrix} \mathbf{K}_{II}^{(L)} & \mathbf{K}_{IL} \\ \mathbf{K}_{LI} & \mathbf{K}_{LL} \end{bmatrix} \begin{bmatrix} \mathbf{u}_I \\ \mathbf{u}_L \end{bmatrix} = \begin{bmatrix} \mathbf{F}_C \\ \mathbf{F}_L \end{bmatrix} \tag{4}$$

where $\mathbf{F}_C = \mathbf{K}_{II}^{(L)}\mathbf{u}_I + \mathbf{K}_{IL}\mathbf{u}_L$

It is important to note that the physical meaning of $\mathbf{F}_C$ is the vector of internal forces that occur at the interface between the upper and lower substructures. $\mathbf{F}_C$ couples two decomposed system of equations into assembled one. Since the reinforcing member is additionally designed on the existing structure, interface nodes would be some nodes of the existing structure model. Therefore, additional calculation of stiffness matrix of the existing structure is not required, and the existing structure model with a little modification of boundary conditions can be used. Above decomposition procedure can also be performed on the models of commercial finite element analysis software. Tasks needed to be done on the both substructure models are identifying node numbers on interfaces and applying corresponding boundary conditions on them. Therefore,

the decomposition scheme can be easily applicable to real industrial fields.

On the other hand, non-linear models such as models with material and geometrical non-linearity can be expected to be decomposed in the same way as the linear models. It is necessary to follow above decomposition procedure steps considering their non-linearities in the system of equations. Based on the decomposed system of equations, independent analyses of the upper and lower substructures can be conducted.

2.2 Analysis of the existing structure

Based on the decomposition explained in Section 2.1, the system of equations for the upper substructure, i.e., the existing structure, is expressed as follows (5):

$$\begin{bmatrix} \mathbf{K}_{UU} & \mathbf{K}_{UI} \\ \mathbf{K}_{IU} & \mathbf{K}_{II}^{(U)} \end{bmatrix} \begin{bmatrix} \mathbf{u}_U \\ \mathbf{u}_I \end{bmatrix} = \begin{bmatrix} \mathbf{F}_U \\ \mathbf{F}_I - \mathbf{F}_C \end{bmatrix} \tag{5}$$

As shown on the left side of Fig. 2, a lower substructure is removed from the upper substructure, and $\mathbf{F}_C$ is added as an additional external force at interface nodes. From the structural perspective, $\mathbf{F}_C$ expresses the stiffness of the lower substructure. Therefore, if $\mathbf{F}_C$ accurately expresses the behavior of a lower substructure, the global behavior of the upper substructure without the lower substructure will be exactly that of the upper substructure in an assembled structure. The precise value of $\mathbf{F}_C$ that produces consistency between the upper and lower substructures is determined through an MDO method, as described in Section 3.

The analysis model of the upper substructure consists of elements that belong only to the upper substructure. Nodes which are only belong to the upper substructure and on interfaces are considered in an analysis of the upper substructure. The boundary conditions of the upper substructure consist of two parts. The first is the original boundary condition of the assembled structure, which is imposed on the upper substructure. This typically consists of a Dirichlet boundary condition, which represents constraints of the assembled structure, and a Neumann boundary condition, which represents the external forces applied to the assembled structure. The other boundary condition is a Neumann boundary condition that represents the stiffness of the lower substructure. The results of the analysis also consist of two parts. The first is a performance measure of the assembled structure, containing quantities that represent the performances of the structure such as the stiffness, compliance, and stress. Such performances are considered as design objectives or constraints of the assembled structure. The other analysis result involves the displacement of nodes on interfaces. This displacement defines the target stiffness of the lower substructure and is utilized as a boundary condition in the lower substructure analysis to ensure consistency between the designs of the upper and lower substructures. A detailed description of the lower substructure boundary conditions and their optimization are presented in Sections 3 and 2.3. The proposed model, boundary conditions, and results of an analysis of the upper substructure are summarized in Table 1.

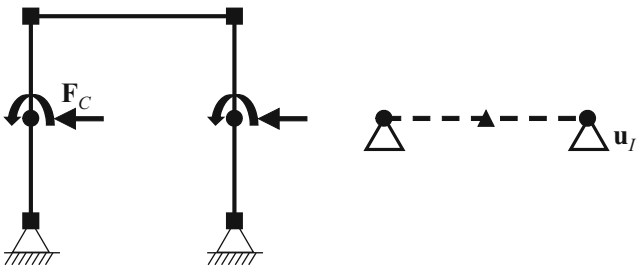

Fig. 2 Additional boundary conditions for upper (left) and lower (right) substructures

2.3 Analysis of the reinforcing member

As with the upper substructure, and based on the decomposition described in Section 2.1, a system of equations for the lower substructure, i.e., the reinforcing member, can be expressed through (6).

$$\begin{bmatrix} \mathbf{K}_{II}^{(L)} & \mathbf{K}_{IL} \\ \mathbf{K}_{LI} & \mathbf{K}_{LL} \end{bmatrix} \begin{bmatrix} \mathbf{u}_I \\ \mathbf{u}_L \end{bmatrix} = \begin{bmatrix} \mathbf{F}_C \\ \mathbf{F}_L \end{bmatrix} \tag{6}$$

Figure 2 shows the physical meaning of the system of equations for the lower substructure. Here, $\mathbf{F}_C$ is the internal force at interface nodes in assembled structure, and part of the external force propagated from the upper to the lower substructure. $\mathbf{u}_I$ is the displacement of interface nodes for the lower substructure according to $\mathbf{F}_C$. Therefore, $\mathbf{u}_I$ and $\mathbf{F}_C$ represent the stiffness of the lower substructure, which affects the behavior of the upper substructure. Therefore, for consistency in the analysis results of the upper and lower substructures, the exact values of $\mathbf{u}_I$ and $\mathbf{F}_C$ should be determined. To determine the exact values, $\mathbf{u}_I$ and $\mathbf{F}_C$ will

Table 1 Details of upper substructure analysis

	Description
Model	Upper substructure only, without lower substructure
B.C.	Original B.C. imposed on upper substructure
	Neumann B.C. representing stiffness of lower substructure, $\mathbf{F}_C$
Result	Performance measure of upper substructure
	Displacement of interface nodes which will be allocated to lower substructure, $\mathbf{u}_I$

be utilized as a linking variable of optimization, as described in Section 3.

As with the upper substructure, an analysis model of the lower substructure consists of elements that belong only to the lower substructure. Nodes considered in the analysis are those that belong to the lower substructure and are located at the interface. The boundary conditions of the analysis also consist of two parts. The first condition is the original boundary condition imposed on the lower substructure. However, typical boundary conditions such as constraints and external forces are not directly applied to the lower substructures since reinforcing members are additively designed and they are located inside of the upper substructure. Therefore, for an independent analysis, the second part of the boundary condition should be determined considering the possibility that the first part of the boundary condition may be absent. The second boundary condition can be imposed based on the external force propagated through the upper substructure. The propagated force can be expressed as either the displacement of interface nodes ($\mathbf{u}_I$) or the internal force applied to these nodes ($\mathbf{F}_C$). As mentioned above, if no constraints are originally applied to the lower substructure, an independent analysis cannot be conducted using only the internal force $\mathbf{F}_C$ because the structure is not constrained. Therefore, to make an independent analysis possible, $\mathbf{u}_I$ is utilized as a Dirichlet boundary condition in the form of an enforced displacement.

Because $\mathbf{u}_I$, i.e., the displacement of interface nodes, is an enforced displacement boundary condition of the analysis, the results of the analysis constitute the reaction force at these nodes. This force has the same physical meaning as the internal force $\mathbf{F}_C$. Therefore, if $\mathbf{F}_C$ resulting from an analysis of the lower substructure has the same value as $\mathbf{F}_C$, which is used as a boundary condition of the upper substructure, consistency between two independent analyses can be established. To summarize, $\mathbf{u}_I$ is the analysis result for the upper substructure, and used as a Dirichlet boundary condition in the lower substructure at the same time. Conversely, $\mathbf{F}_C$ is used as a Neumann boundary condition in the upper substructure, and appears as a result of the analysis in the lower substructure. The optimization process of matching $\mathbf{u}_I$ and $\mathbf{F}_C$ between two independent analyses is described in Section 3. The model, boundary conditions, and results of analysis of the lower substructure are summarized in Table 2.

Table 2 Details of lower substructure analysis

	Description
Model	Lower substructure only
B.C.	Enforced displacement of Dirichlet B.C. allocated from upper substructure, $\mathbf{u}_I$
Results	Performance measure of lower substructure
	Reaction force at interface nodes representing stiffness of lower substructure, $\mathbf{F}_C$

2.4 Target stiffness of the reinforcing member

Based on the decomposition results, the target stiffness of the lower substructure, i.e., the reinforcing member, can be defined based on the force applied to the member and the displacement produced by such force. The target stiffness of the reinforcing member consists of $\mathbf{F}_C$ and $\mathbf{u}_I$. The displacement is utilized as a boundary condition of the reinforcing member and can be utilized as an evaluation method. The reaction force and analysis results for the reinforcing member compose a quantification metric for the stiffness of the member. To allocate the target stiffness to the member, $\mathbf{F}_C$ and the resulting $\mathbf{u}_I$ will be analyzed and determined in the optimization of the existing structure. At the reinforcing member level, the design details for the member that satisfy the allocated target stiffness will be determined. If the method is applied for dynamic models, $\mathbf{F}_C$ and $\mathbf{u}_I$ of every time step of the analysis should be considered to achieve consistency between decomposed models. Therefore, target stiffness is defined by using $\mathbf{F}_C$ and $\mathbf{u}_I$ of every time step to extend the method to dynamic models. Details of the derivation of the optimal target stiffness are described in Section 3.

3 Optimization and allocation of target stiffness

In this section, an optimization scheme and a detailed formulation are described to find the optimal target stiffness and design for the reinforcing member. Description of the target stiffness allocation problem is supplied in Section 3.1. For a systematic optimization of the structure, a modified ATC method is employed. In Section 3.2, a brief introduction of the ATC method with a quadratic penalty function is described. In Section 3.3, details of the optimization scheme and associated formulations are described.

3.1 Description of the target stiffness allocation problem

Through the decomposition presented in Section 2, the target stiffness is defined based on decomposed models of the existing structure and reinforcing member. The objective is to find optimum target stiffness and design of the reinforcing member which maximize performance of the existing structure. In the existing structure, target

stiffness of the reinforcing member is the only variables which need to be determined. The structure has design requirements such as compliance and displacement which need to be maximized, minimized, or within specified boundary according to the requirements. Design problem of the target stiffness can be defined as following formulation:

$$\begin{aligned} &\min_{\mathbf{F}_C} \quad f_{\text{obj},U}\left(\mathbf{F}_C\right) \\ &\text{s.t.} \quad \mathbf{g}_U\left(\mathbf{F}_C\right) \le 0 \end{aligned} \tag{7}$$

where $f_{\text{obj},U}$ and $\mathbf{g}_U$ represent objective function and design requirements of the existing structure, respectively.

In the reinforcing member, geometric dimensions such as radius, thickness, and length are design variables that need to be determined. The member also has its design objective and requirements such as mass. Thus, design problem of the reinforcing member is defined as follows:

$$\begin{aligned} &\min_{\mathbf{x}_L} \quad f_{\text{obj},L}\left(\mathbf{x}_L\right) \\ &\text{s.t.} \quad \mathbf{g}_L\left(\mathbf{x}_L\right) \le 0 \end{aligned} \tag{8}$$

where $f_{\text{obj},L}$ and $\mathbf{g}_L$ represent objective function and design requirements of the reinforcing member, respectively. It is important to note that coupling variable $\mathbf{F}_C$ in (7) is calculated through the reinforcing member as a function of its design variables, $\mathbf{x}_L$.

The target stiffness problem consists of two subproblems with their own formulations. The problem has following characteristics. First, each formulation represents physical objects, and they are under hierarchical relationship. The reinforcing member physically belongs to the existing structure, and multiple reinforcing members can be attached to a single existing structure. Second, $\mathbf{F}_C$ exists in both existing structure and reinforcing member. Thus, individual optimization of each formulation cannot guarantee consistency of the variable. Therefore, concurrent design methodology such as MDO is needed. Third, the target stiffness is design variable in the existing structure, while it is the response in the reinforcing member.

3.2 Analytical target cascading

ATC is an MDO method developed for optimization of multidisciplinary systems with a hierarchical structure. ATC has following main characteristics. First, it derives the optimal design of entire systems by repeating separate optimization of each individual discipline. Owing to this feature, ATC is suitable for hierarchical system that consists of the object oriented disciplines (Allison 2004). Second, consistency of linking variables achieved by minimizing penalty function. Third, target linking variables of lower discipline are derived as a result of optimization. In an upper level discipline, these linking variables are treated as design variables of the optimization problem. In lower level disciplines, the same linking variables are discipline responses, which are derived from a discipline analysis. Since these features coincide with the characteristics of the problem, ATC is the most suitable MDO method and is applied to the problem at hand.

An ATC optimization scheme is shown in Fig. 3. One component is located under a single upper level discipline, and several lower level disciplines are followed by the component. Linking variables representing the targets exist between the disciplines at different levels. Many modified methods to improve the convergence property of the original ATC method are available (Li et al. 2008; Michalek and Papalambros 2005). In this study, an ATC method using a quadratic penalty function, which has been widely used, is employed (Tosserams et al. 2006). The optimization formulation used for the general disciplines is shown in (9).

$$\begin{aligned} &\min_{\bar{\mathbf{x}}_{ij}} \quad f_{ij}\left(\bar{\mathbf{x}}_{ij}\right) + \pi\left(\mathbf{c}_{ij}\right) + \sum_{k \in l_{ij}} \pi\left(\mathbf{c}_{(i+1)k}\right) \\ &\qquad = f_{ij}\left(\bar{\mathbf{x}}_{ij}\right) + \left\| \mathbf{w}_{ij}^T \mathbf{c}_{ij} \right\|^2 + \sum_{k \in l_{ij}} \left\| \mathbf{w}_{(i+1)k}^T \mathbf{c}_{(i+1)k} \right\|^2 \\ &\text{s.t.} \quad \mathbf{g}_{ij}\left(\bar{\mathbf{x}}_{ij}\right) \le 0 \\ &\qquad \mathbf{h}_{ij}\left(\bar{\mathbf{x}}_{ij}\right) = 0 \\ &\qquad \bar{\mathbf{x}}_{ij} = \left[\mathbf{x}_{ij}, \mathbf{r}_{ij}, \mathbf{t}_{(i+1)k_1}, \cdots, \mathbf{t}_{(i+1)k_n}\right] \\ &\qquad \mathbf{c}_{ij} = \left(\mathbf{t}_{ij} - \mathbf{r}_{ij}\right) \end{aligned} \tag{9}$$

f_{ij}, g_{ij}, and h_{ij} represent the original objective function, inequality constraint, and equality constraint, respectively. In an objective function, a quadratic penalty function, $\pi\left(\mathbf{c}_{ij}\right)$, is added to the original objective function to make the linking variables consistent over the disciplines. $\mathbf{c}_{ij}$ represents the inconsistency of the linking variable and will be minimized as the optimization is carried out. w is the

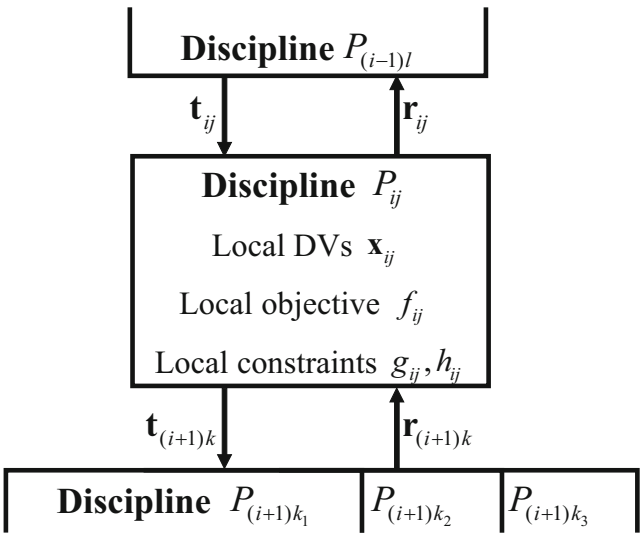

Fig. 3 ATC formulation for hierarchical system

penalty weight for the quadratic function and is updated at every iteration. The updating rule for the penalty weight is shown in (10).

$$w^{(\kappa+1)} = \beta w^{(\kappa)} \tag{10}$$

where β is an updating parameter and a value of between 2 and 3 is usually assigned. Convergence of the ATC is evaluated based on an inconsistency in the linking variables. If the maximum inconsistency of the linking variables is smaller than the specified tolerance, the optimization is terminated. The mathematical convergence criterion is expressed through (11).

$$\max\left(\left|\mathbf{c}_{ij}^{(\kappa)}\right|\right) \leq \varepsilon \tag{11}$$

3.3 Optimization scheme and formulation

Optimization is conducted using a modified ATC. The input and output of each level and optimization scheme are described in Fig. 4. At the existing structure level, the design objective and constraints of the assembled structure are considered as a response. Here, $\mathbf{F}_C$ is employed as a design variable to determine the target stiffness of the reinforcing member, considering both the objective and constraints. As $\mathbf{F}_C$ is determined, $\mathbf{F}_C$ and $\mathbf{u}_I$ are allocated to the reinforcing member as a target stiffness. At the reinforcing member level, the target stiffness and design objective, such as the mass, are considered as a response. The allocated displacement, $\mathbf{u}_I$, is utilized as a Dirichlet boundary condition of the analysis. If the resulting reaction force is the same as the allocated $\mathbf{F}_C$, the reinforcing member satisfies the target stiffness. Unlike the typical ATC method, among the allocated linking variables, only $\mathbf{F}_C$ is sent back to the existing structure level. This is because an analysis of the existing structure is a bijective function of $\mathbf{F}_C$ and $\mathbf{u}_I$. Therefore, consistency between levels can be guaranteed using only $\mathbf{F}_C$, which is a difference between the original ATC and the proposed method. An optimization formulation of the existing structure level is shown in (12).

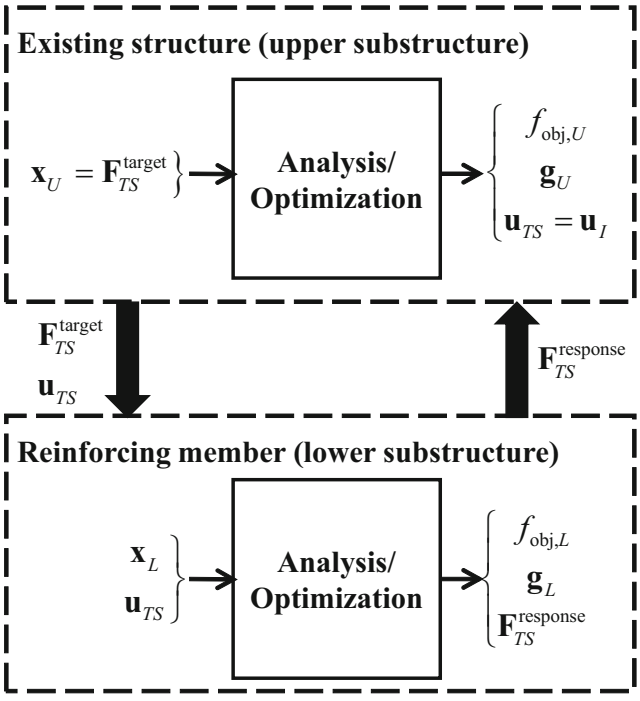

Fig. 4 Optimization scheme for target stiffness allocation

$$\begin{aligned} \min_{\mathbf{x}_U} \quad & \left\| \mathbf{w}^{(\kappa)T} \left(\mathbf{F}_{TS}^{\text{target}} - \mathbf{F}_{TS}^{\text{response}} \right) \right\|^2 + f_{\text{obj},U}\left(\mathbf{x}_U\right) \\ \text{s.t.} \quad & \mathbf{g}_U\left(\mathbf{x}_U\right) \leq 0 \\ \text{where} \quad & \mathbf{x}_U = \mathbf{F}_{TS}^{\text{target}} \end{aligned} \tag{12}$$

For the reinforcing member level, optimization is conducted under the formulation shown in (13). Here, $\mathbf{F}_{TS}$ and $\mathbf{u}_{TS}$ represent allocated value of the target stiffness $\mathbf{F}_C$ and $\mathbf{u}_I$, respectively. A flowchart of the optimization process is shown in Fig. 5.

$$\begin{aligned} \min_{\mathbf{x}_L} \quad & \left\| \mathbf{w}^{(\kappa)T} \left(\mathbf{F}_{TS}^{\text{target}} - \mathbf{F}_{TS}^{\text{response}}\left(\mathbf{x}_L\right) \right) \right\|^2 + f_{\text{obj},L}\left(\mathbf{x}_L\right) \\ \text{s.t.} \quad & \mathbf{g}_L\left(\mathbf{x}_L\right) \leq 0 \\ \text{where} \quad & \mathbf{x}_L = \left[r_1, t_1, l_1, \cdots \right] \end{aligned} \tag{13}$$

Each optimization problem can be solved by using gradient-based optimization algorithms, where gradient information is calculated by using finite difference method in this research.

4 Examples

In this section, the proposed method is applied to two examples, namely reinforcing members of the portal frame and BIW of the vehicle, and the results are discussed.

4.1 Portal frame with reinforcing member

A simple portal frame, which is detailed in Section 2 to describe the proposed method, is employed using a detailed description and formulations.

4.1.1 Problem description

A simple portal frame described in Fig. 6 is considered. Assume that structure A is under external forces applied from the side of the structure. To improve the rigidity, structure B is added to structure A as a reinforcing member. The objective of the design is finding a target stiffness and a lightweight design of structure B, considering the required rigidity of the assembled structure.

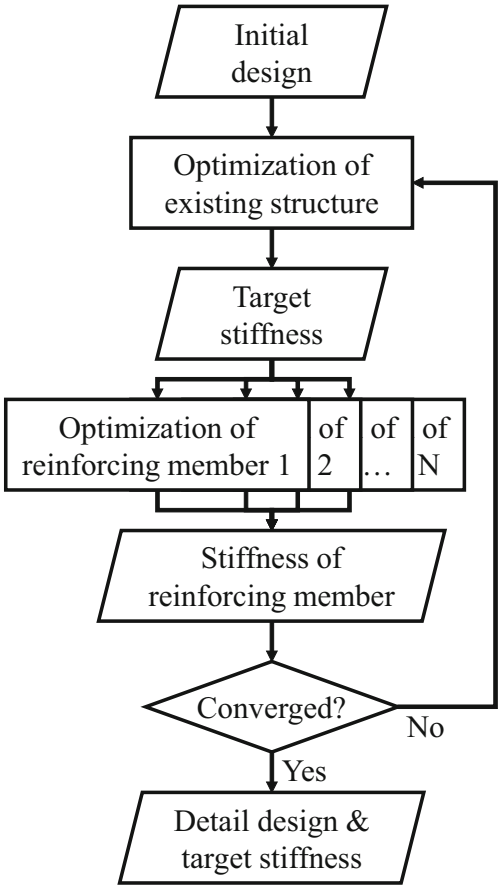

Fig. 5 Flow chart of target stiffness allocation

Both structures consist of beam elements with pipe cross-sections. The cross-section of structure A has an outer radius of 15 mm and a thickness of 1 mm. The outer radius and thickness of the cross-section of structure B are design variables. The design boundary of the radius and the thickness are 7.5 to 22.5 mm and 0.5 to 1.5 mm, respectively. The design objective is to find a target stiffness and a lightweight design for the reinforcing member that satisfies the design requirements. The design requirement is achieving the displacement of node 4 less than 12 mm. Dimensions, cross-section, external force, and node numbers are expressed in Fig. 6.

4.1.2 Analysis and formulation

An analysis diagram of the structures is supplied in Fig. 7. To simplify the optimization problem, some elements of the force and displacement are neglected considering the characteristics of the structure. Because a deformation of the structure occurs in the x–y plane, F_z, M_x, and M_y are not considered. The target stiffness of structure B is defined by F_y, M_z, u_y, and θ_z of nodes 1 and 2 considering the structural symmetry. System of equations of structures are developed based on Euler–Bernoulli beam theory and implemented in MATLAB code. The boundary conditions and results of the analysis of each structure are described in Table 3.

Neumann boundary conditions representing the stiffness of structure B are applied to structure A. As a result, the displacements of nodes are calculated through an analysis. The displacement of node 4 is used to evaluate the design requirements of the structure. In addition, the displacements of nodes 1 and 2 are allocated to structure B as a target stiffness. In structure B, the allocated displacement is applied as a Dirichlet boundary condition. The reaction force at nodes 1 and 2 and the mass of structure B are calculated through an analysis. The reaction force is used to evaluate the stiffness of structure B. The mass of structure B is a design objective. An optimization formulation and a scheme for MDO are expressed in Fig. 8. Convergence

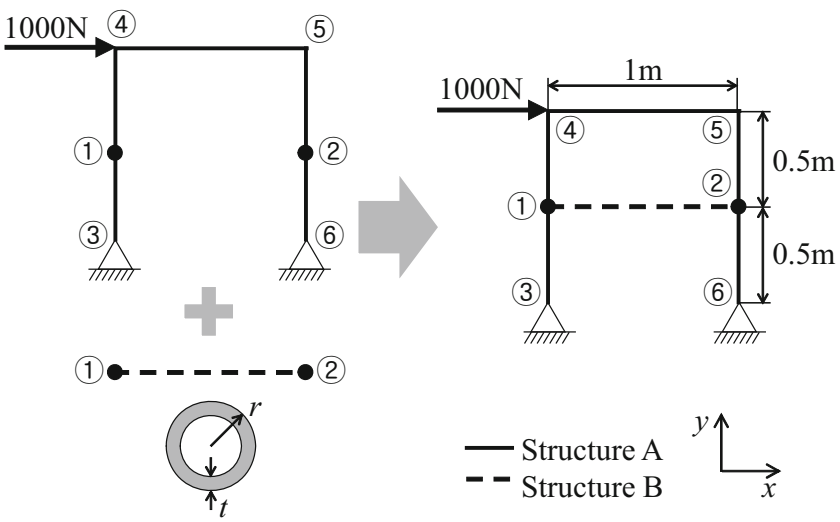

Fig. 6 Details of the portal frame example

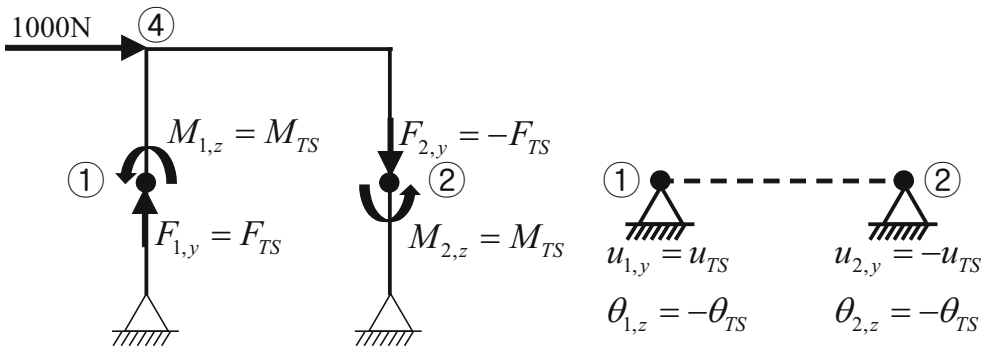

Fig. 7 Additional boundary conditions for structures

criterion of optimization is expressed in (14) and $\varepsilon = 0.01$ is used. F_{TS}^0 and M_{TS}^0 are parameters for normalization.

$$\max \left\{ \left| \frac{F_{TS}^{\text{target}} - F_{TS}^{\text{response}}}{F_{TS}^0} \right|, \left| \frac{M_{TS}^{\text{target}} - M_{TS}^{\text{response}}}{M_{TS}^0} \right| \right\} \leq \varepsilon \tag{14}$$

Additionally, to verify optimization result of the proposed method, the problem is solved by using IDF method (Cramer et al. 1994) which is one of the most popular MDO methods. Optimization formulation for IDF method is given as follows:

$$\begin{aligned} \min_{\mathbf{x}} \quad & m_B(\mathbf{x}) \\ \text{s.t.} \quad & g_A(\mathbf{x}) = \delta_4 \leq 12 \\ & F_{TS} - \bar{F}_{TS}(\mathbf{x}) = 0 \\ & M_{TS} - \bar{M}_{TS}(\mathbf{x}) = 0 \\ & u_{TS} - \bar{u}_{TS}(\mathbf{x}) = 0 \\ & \theta_{TS} - \bar{\theta}_{TS}(\mathbf{x}) = 0 \end{aligned} \tag{15}$$

where $\mathbf{x} = \left[F_{TS}, M_{TS}, u_{TS}, \theta_{TS}, r, t \right]$

4.1.3 Results

Based on the optimization formulation, the optimal design and target stiffness of the structure are determined. A penalty weight of 2 is used to update parameter β. The optimum design and target stiffness of the structure are shown in Table 4. With the initial design, the structure does not satisfy the design requirement, i.e., displacement at node 4. After optimization, the constraint is satisfied. The mass of structure B, which is a design objective of the problem, is also reduced by 9.91% compared with the initial design. The design variables and target stiffness for structure B satisfying these performance measures are also derived.

To verify the result, it is observed that the proposed method and IDF converged to identical design with 0.7% of maximum relative difference. The difference can be caused by the way of synchronizing linking variables, i.e., ATC uses penalty objective function, while IDF uses equality constraint. Thus, the difference can be reduced by reducing convergence tolerance ε.

Table 5 shows the convergence of the linking variables for structures A and B, i.e., the target stiffness for structure B. The target column represents the target stiffness allocated from structures A to B. The response column represents the actual stiffness of structure B. As the optimization proceeds, the discrepancy between the target and response becomes smaller. At the 8th iteration, the convergence criterion is satisfied and the linking variables F_{TS} and M_{TS} are converged.

4.1.4 Independent design of the reinforcing member using target stiffness

Based on the target stiffness, a detailed design of the reinforcing member can be conducted rapidly and at

Table 3 Boundary condition and results of analysis of structures in the portal frame example

		Description	Symbols
Existing structure (structure A)	B.C.	Original B.C.; fixed constraint and external forces	–
		Neumann B.C. representing lower substructure	F_{TS}^{target}, M_{TS}^{target}
	Result	Performance measure, displacement (constraint)	δ_4
		Displacement of interface nodes	u_{TS}, θ_{TS}
Reinforcing member (structure B)	B.C.	Enforced displacement Dirichlet B.C.	u_{TS}, θ_{TS}
	Result	Performance measure; mass (objective)	m_B
		Reaction force at interface nodes	F_{TS}^{response}, M_{TS}^{response}

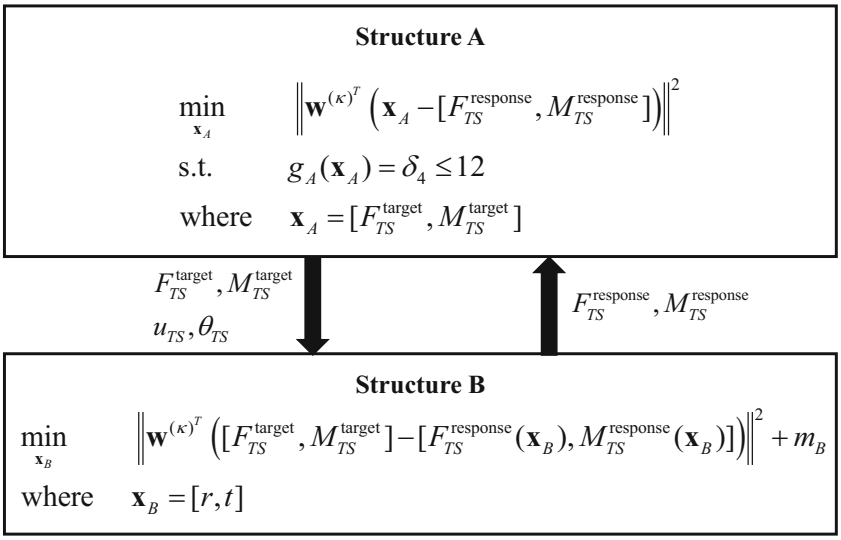

Fig. 8 Optimization scheme of the portal frame example

Table 4 Formulation and results of the portal frame example

	Symbol	Description	Formulation	Initial	Optimum		Remarks	Unit
					Proposed	IDF		
Objective	m_B	Mass of structure B	Minimize	0.7106	0.6402	0.6425	9.91%↓	kg
Constraint	δ_4	Displacement of node 4	≤ 12	15.42	12.00	12.00	Active	mm
Design variables	r	Radius of cross-section of structure B	[7.5, 22.5]	15.00	22.50	22.50	Active	mm
	t	Thickness of cross-section of structure B	[0.5, 1.5]	1.000	0.5883	0.5904	Satisfied	mm
Target stiffness	u_{TS}	Displacement of interface nodes		1.650e-2	1.770e-2	1.778e-2		mm
	θ_{TS}			1.473e-2	8.649e-3	8.649e-3		rad
	F_{TS}	Reaction force at interface nodes		355.2	437.8	440.9		N
	M_{TS}			177.6	220.4	220.4		Nm

Table 5 Convergence of target stiffness during the optimization process in the portal frame example

Iteration	F_{TS}			M_{TS}		
	Target (N)	Response (N)	Relative error (%)	Target (Nm)	Response (Nm)	Relative error (%)
1	355.10	352.55	0.720	220.41	176.27	20.0
2	352.50	375.88	6.63	220.41	187.94	14.7
3	375.85	399.97	6.42	220.42	199.98	9.27
4	399.95	418.30	4.59	220.43	209.15	5.12
5	418.29	429.05	2.57	220.43	214.53	2.68
6	429.04	434.83	1.35	220.43	217.41	1.37
7	434.82	437.81	0.688	220.44	218.91	0.694
8	437.81	439.34	0.348	220.44	219.67	0.349

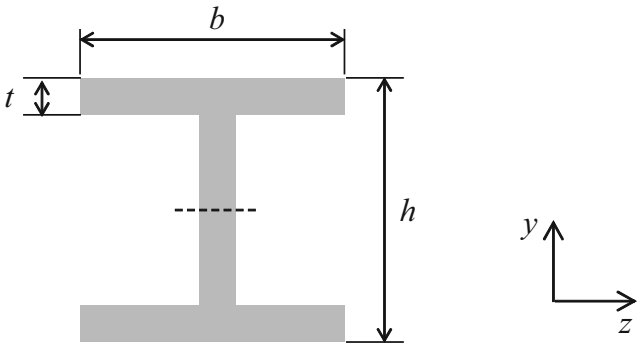

Fig. 9 Cross-section of the I-beam reinforcing member

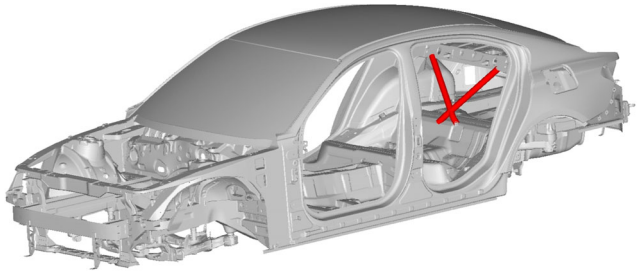

Fig. 10 Finite element model of BIW (gray) and reinforcing member (red)

little cost. Without the target stiffness, an analysis of the assembled structure is necessary for re-design of structure B. However, by utilizing the target stiffness, the design can be carried out using only an analysis of structure B. To verify the derived target stiffness, structure B is re-designed with an I-beam. Structure B is analyzed using the enforced displacement boundary conditions of u_{TS}^{opt} and θ_{TS}^{opt}, as shown in Fig. 7. The cross-section of the beam is shown in Fig. 9. The design variables are the height of the web, the width of the flange, and the thickness of the web and flange. The design objective is finding the lightest beam design that satisfies the derived target stiffness. An optimization formulation is shown in (16).

$$\begin{aligned} \min_{\mathbf{x}_B} \quad & m_B(\mathbf{x}_B) \\ \text{s.t.} \quad & F_y(\mathbf{x}_B) \geq F_{TS}^{\text{opt}} = 437.8 \\ & M_z(\mathbf{x}_B) \geq M_{TS}^{\text{opt}} = 220.4 \end{aligned} \tag{16}$$

where $\mathbf{x}_B = [\, h, b, t \,]$

To address accuracy and cost reduction of the independent design, the structure B with I-beam is optimized by using IDF method in the same way as shown in (15), and results are compared. The optimization results are supplied in Table 6. The weight of the structure is reduced while satisfying the target stiffness as an active constraint. Structure B with an optimal cross-section, which is designed independently of structure A, is assembled into structure A and analyzed to verify whether the design requirement for a assembled portal frame is satisfied. As shown in Table 6, the displacement of node 4 in assembled structure is reduced from 13.42 to 12.00 mm and the design requirement is satisfied.

Compared to result of the IDF method, which optimizes the structure A and B simultaneously, both approaches converged to identical design result. This result shows that the identical design can be derived by using the target stiffness without employing existing structure model. Therefore, the target stiffness calculated through the proposed method is reasonable and accurate guideline for independent design of reinforcing member. Additionally, as shown in Table 6, the independent design saved cost for static analysis of the structure A, while the IDF method performed 56 times. Even in case of the structure B, the independent design performed static analysis only 28 times, while the IDF method 56 times. The independent design converged faster than the IDF method because of reduced dimension of the optimization problem. This result shows that the identical result can be derived rapidly and at little cost by using target stiffness.

Table 6 Optimization results of the I-beam reinforcing member

	Symbol	Formulation	Initial	Optimum		Remark	Unit
				Independent design	IDF		
Objective	m_B	Minimize	0.6864	0.4357	0.4357	36.5%↓	kg
Constraint	F_y	$\geq F_{TS}^{\text{opt}} = 437.8$	313.6	440.9	440.9	Satisfied	N
	M_z	$\geq M_{TS}^{\text{opt}} = 220.4$	156.8	220.4	220.4	Active	Nm
Design variables	h	[15, 45]	30.00	45.00	45.00	Active	mm
	b	[15, 45]	30.00	33.86	33.86	Satisfied	mm
	t	[0.5, 1.5]	1.000	0.5000	0.5000	Active	mm
Assembled structure	δ_4	≤ 12	13.42	12.00	12.00	*Satisfied*	mm
# of structure A analysis				0	56		Times
# of structure B analysis				28	56		Times

Table 7 Boundary condition and results of analysis of BIW and reinforcing member

		Description	Symbol
BIW	B.C.	Original B.C.; B.C. for torsional stiffness evaluation	–
		Neumann B.C. representing reinforcing member	$\mathbf{F}_{TS}^{\text{target}}$
	Result	Performance measure, torsional stiffness (constraint)	k_{torsion}
		Displacement of interface nodes	$\mathbf{u}_{TS}$
Reinforcing member	B.C.	Enforced displacement Dirichlet B.C.	$\mathbf{u}_{TS}$
	Result	Performance measure, mass (objective)	m_{RM}
		Reaction force at interface nodes	$\mathbf{F}_{TS}^{\text{response}}$

4.2 BIW with reinforcing member

The proposed method is applied to the design of a reinforcing member of a BIW of a vehicle manufactured by Hyundai Motor Company. Using this method, an optimal design and the target stiffness of the reinforcing member are derived.

4.2.1 Problem description

The stiffness of the BIW has a significant effect on the driving performance of the vehicle. A general way to improve the stiffness is to conduct a design optimization of the BIW considering several stiffnesses needed to be improved (Lim et al. 2016). However, it can also be improved by adding some reinforcing members specially designed for improving the specific stiffness to the existing BIW. For example, a front strut tower bar is a well-known reinforcing member for improving the torsional stiffness of a vehicle (Takamatsu et al. 1992) and is widely applied to high-performance vehicles. By utilizing additional reinforcing members, the manufacturer can make vehicles with different trim levels using a single BIW rapidly and at little cost. Because reinforcing members with similar shapes are applied to various vehicle models, and various materials such as aluminum, steel, or carbon fiber reinforced plastic (CFRP) are used for reinforcing members (Lee et al. 2014), a repetitive design of the member is carried out by the member design team. Without a proper target stiffness of the member, an expensive BIW analysis should be conducted for every single design cycle. However, if the target stiffness for the member can be determined and allocated to the team, the design cycle of the member can be reduced.

In this study, a reinforcing member of a vehicle manufactured by Hyundai Motor Company is considered to improve the torsional stiffness. To establish the design guidelines for the reinforcing member, the target stiffness is derived through the proposed method. The design objective is to derive the target stiffness for the reinforcing member that satisfies the required torsional stiffness of a BIW. The reinforcing member is located behind the rear seat. Its shape is determined through a topology optimization that considers the torsional stiffness of the BIW. The ABAQUS FE model of the BIW set by Hyundai Motor Company is utilized to evaluate the torsional stiffness. Figure 10 shows an FE model for a BIW and its reinforcing member. Elements with gray and red color represents the BIW and reinforcing member, respectively.

4.2.2 Analysis and formulation

To apply the proposed method in this example, the BIW and reinforcing member are regarded as the respective upper and lower substructures described in Section 2. As shown in the previous example, an analysis and optimization of the BIW and the reinforcing member are carried out separately. The boundary conditions and results of the analyses are shown in Table 7. Six degrees of freedom of the reaction force and displacement at the nodes (where the reinforcing member is attached) define the target stiffness.

For optimization, the torsional stiffness of the BIW is considered as a constraint at the upper substructure level,

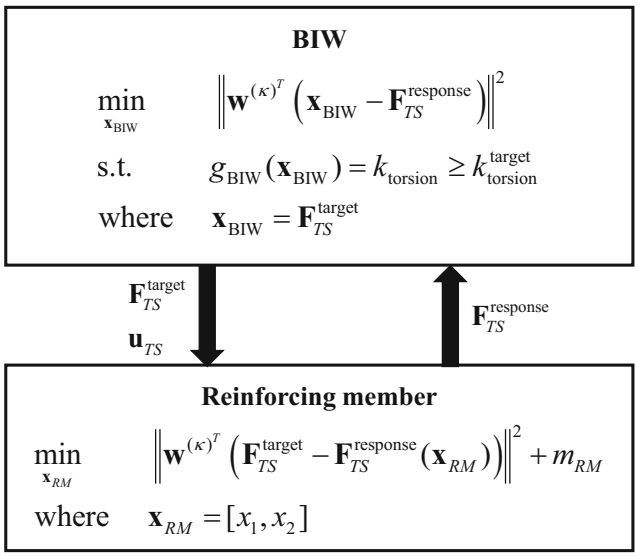

Fig. 11 Optimization scheme and formulation of BIW and reinforcing member

Table 8 Optimization results of the BIW and reinforcing member

	Symbol	Formulation	W/o reinforcing member	With reinforcing member		
				Initial	Optimum	Remarks
Objective	m_{RM}	Minimize	–	1.000	0.3462	65%↓
Constraint	k_{torsion}	$\geq k_{\text{torsion}}^{\text{target}} = 1$	0.9230	1.273	1.263	Satisfied
Design	x_1	[0, 1]	–	0.5000	3.889e-2	Satisfied
variables	x_2	[0, 1]	–	0.5000	0.0000	Active

whereas the mass of the reinforcing member is considered as the objective function at the lower substructure level. Design variables in the lower substructure level are geometric dimensions of the reinforcing member. An optimization formulation is shown in Fig. 11. Details of the evaluation method for the torsional stiffness and the design variables of the reinforcing member are omitted for the purposes of confidentiality. Convergence criterion for the optimization is expressed in (17) and $\varepsilon = 0.01$ is used. $F_{TS,i}^0$ are normalization parameters.

$$\max_{1\leq i\leq 24}\left\{\left|\frac{F_{TS,i}^{\text{target}} - F_{TS,i}^{\text{response}}}{F_{TS,i}^0}\right|\right\} \leq \varepsilon \tag{17}$$

4.2.3 Results

Using the proposed method, an optimal design and the target stiffness of the reinforcing member is determined. Table 8 shows the change in mass of the reinforcing member, torsional stiffness of the BIW, and design variables of the reinforcing member. For the purpose of confidentiality, objective and constraint are normalized with their initial and target value respectively. Design variables are normalized between 0 and 1, which represent lower and upper design boundaries, respectively. At the 17th iteration, the convergence criterion is satisfied and the optimization is terminated. Without a reinforcing member, the BIW does not satisfy the required torsional stiffness constraint. However, with the optimized reinforcing member, the torsional stiffness is increased to the required level. The mass of the reinforcing member is reduced by approximately 65% compared with the initial design. Table 9 supplies the derived target stiffness of the reinforcing member. Although 24 linking variables are considered, all elements of the target stiffness converge with only small discrepancies between levels. Target and response values of $F_{TS,i}$ in the table are normalized between 0 and 1.

Table 9 Optimal target stiffness and discrepancy between levels

	Target (BIW)	Response (reinforcing member)	Absolute error
$F_{TS,1}$	0.5552	0.5545	6.270e-4
$F_{TS,2}$	0.7408	0.7426	1.841e-3
$F_{TS,3}$	0.3576	0.3559	1.704e-3
$F_{TS,4}$	6.141e-2	6.296e-2	1.556e-3
$F_{TS,5}$	0.1087	0.1115	2.753e-3
$F_{TS,6}$	2.945e-4	-1.780e-4	4.725e-4
$F_{TS,7}$	0.5157	0.5177	1.989e-3
$F_{TS,8}$	0.4523	0.4511	1.250e-3
⋮	⋮	⋮	⋮
$F_{TS,24}$	0.1201	0.1227	2.644e-3

5 Conclusion

In this paper, a method of reinforcing member design on a existing structure by allocating the target stiffness is described. To utilize individual models of the structure and its members, a system of equations of the assembled structure is decomposed using a substructuring technique. Additional boundary conditions are introduced to ensure consistency between the models and define the target stiffness of the reinforcing member. The target stiffness of the member is optimized and allocated using an ATC optimization scheme. Using the proposed method, the reasonable target stiffness of the reinforcing member that considers the design requirements of an assembled structure can be determined through an optimization rather than relying on intuition or engineering experience. The derived target stiffness can also be utilized in the independent designs of the reinforcing members.

To assess the validity and effectiveness of the method, a simple portal frame example is employed and the target stiffness of the reinforcing member is derived. The boundary conditions and target stiffness of the structures are defined according to the proposed method. Through 8 iterations of optimization, the target stiffness and design variables of the member are successfully derived. To verify the optimum result, the result is compared with the IDF method and it is observed that both method obtained identical design. To assess accuracy of the derived target stiffness, an independent design of the reinforcing member

with another cross-section, i.e., an I-beam, is conducted by applying the target stiffness and boundary conditions. The resulting I-beam reinforcing member satisfies the design requirements of the structure, without access of the existing structure. Accuracy and cost reduction of the independent design are shown by comparing with the IDF method. It is shown that independent design using the target stiffness derives identical design with the IDF method. Through an example, accuracy and effectiveness of the target stiffness are verified.

The method is applied to the design of a reinforcing member in a BIW of a vehicle manufactured by Hyundai Motor Company. The optimal design and target stiffness of a reinforcing member that considers the torsional stiffness of the BIW are determined through the proposed method. Although 24 linking variables are considered to define the target stiffness, all linking variables converge with reasonable discrepancies among levels, and the stiffness targets for a reinforcing member are successfully produced, verifying the effectiveness of the method in a large-scale practical problem.

In this paper, the propose method is demonstrated by using linear static models to provide a clear explanation of idea and overall procedure. However, the method can be extended into non-linear and dynamic models. To do this, non-linearity in the system of equations should be carefully assessed in the decomposition process step by step. The target stiffness and the linking variables in the ATC should be defined to consider every time step in dynamic analysis. This procedure depends on characteristics of the analysis such as type of non-linearity. Therefore, the extension should be conducted with models of specific type of the analysis.

Acknowledgments Some contents of this research are part of the "Multidisciplinary design optimization of vehicle body reinforce members" funded by Hyundai Motor Company. The authors appreciate the partial financial support from Hyundai Motor Company.

Funding information This research is partially and financially supported by Hyundai Motor Company.

Compliance with ethical standards

Conflict of interests The authors declare that they have no conflict of interest.

Replication of results For the purpose of replication of results, MATLAB codes of the portal frame example presented in Section 4.1 are provided as a supplementary material. Codes include static analysis of the portal frame, target stiffness allocation, re-design of the structure B with I-beam cross-section, and optimization using IDF method. MATLAB 2018b was used to generate the results. Codes and files related to vehicle BIW example presented in Section 4.2 cannot be provided for the purposes of confidentiality.

References

Adams V (2008) A designer's guide to simulation with finite element analysis. NAFEMS, Hamilton

Allison JT (2004) Complex system optimization: a review of analytical target cascading, collaborative optimization, and other formulations. Master's thesis University of Michigan, Ann Arbor

Austin-Breneman J, Honda T, Yang MC (2012) A study of student design team behaviors in complex system design. J Mech Des 134(12):124504

Braun RD (1997) Collaborative optimization: an architecture for large-scale distributed design. Dissertation Stanford University, Stanford

Cramer EJ, Dennis JJE, Frank PD, Lewis RM, Shubin GR (1994) Problem formulation for multidisciplinary optimization. SIAM J Optimiz 4(4):754–776

Kang N, Kokkolaras M, Papalambros PY, Yoo S, Na W, Park J, Featherman D (2014) Optimal design of commercial vehicle systems using analytical target cascading. Struct Multidisc Optim 50(6):1103–1114

Kim HM (2001) Target cascading in optimal system design. Dissertation University of Michigan, Ann Arbor

Kim HM, Rideout DG, Papalambros PY, Stein JL (2003) Analytical target cascading in automotive vehicle design. J Mech Des 125(3):481–489

Kim S, Lim W, Kim H, Ryu N, Kwon K, Lim S, Min S, Lee TH (2016) Robust target cascading for improving firing accuracy of combat vehicle. J Mech Sci Tech 30(12):5577–5586

Kokkolaras M, Louca L, Delagrammatikas G, Michelena N, Filipi Z, Papalambros P, Stein J, Assanis D (2004) Simulation-based optimal design of heavy trucks by model-based decomposition: an extensive analytical target cascading case study. Int J Heavy Veh Syst 11(3-4):403–433

Lee HC, Jung YS, Oh HJ, Kim SS (2014) Design of a hybrid composite strut tower for use in automobiles. Adv Compos Mater 23(3):275–291

Li Y, Lu Z, Michalek JJ (2008) Diagonal quadratic approximation for parallelization of analytical target cascading. J Mech Des 130(5):051402

Lim W, Jang J, Kim S, Lee TH, Kim J, Lee K, Lee C, Kim Y (2016) Reliability-based design optimization of an automotive structure using a variable uncertainty. P I Mech Eng D-J Aut 230(10):1314–1323

Martins JR, Lambe AB (2013) Multidisciplinary design optimization: a survey of architectures. AIAA J 51(9):2049–2075

Michalek JJ, Papalambros PY (2005) An efficient weighting update method to achieve acceptable consistency deviation in analytical target cascading. J Mech Des 127(2):206–214

Sobieszczanski-Sobieski J (1988) Optimization by decomposition: a step from hierarchic to non-hierarchic systems. Tech. Rep. NASA-TM-101494, NASA Langley Research Center

Sobieszczanski-Sobieski J, Agte JS, Sandusky RR (2000) Bilevel integrated system synthesis. AIAA J 38(1):164–172

Takamatsu M, Fujita H, Inoue H, Kijima M (1992) Development of lighter-weight, higher-stiffness body for new RX-7. Tech. Rep. 920244, SAE International

Tosserams S, Etman L, Papalambros P, Rooda J (2006) An augmented lagrangian relaxation for analytical target cascading using the alternating direction method of multipliers. Struct Multidisc Optim 31(3):176–189

Tosserams S, Kokkolaras M, Etman L, Rooda J (2010) A nonhierarchical formulation of analytical target cascading. J Mech Des 132(5):051002

Yang M, Liang XF (2011) Structural reinforced parts for improving roof crush performance. Adv Mat Res 189:391–394

Zienkiewicz OC, Taylor RL, Nithiarasu P, Zhu J (1977) The finite element method, vol 3. McGraw-hill, London